COMPDYN 2015
5th ECCOMAS Thematic Conference on
Computational Methods in Structural Dynamics and Earthquake Engineering
M. Papadrakakis, V. Papadopoulos, V. Plevris (eds.)
Crete Island, Greece, 25–27 May 2015

A MIXED SPACE-TIME AND WAVENUMBER DOMAIN MODEL FOR PREDICTING GROUND VIBRATION FROM SURFACE RAILWAY TRACKS (COMPDYN 2015)

Samuel G. Koroma[1], David J. Thompson[1], Mohammed F.M. Hussein[2] and Evangelos Ntotsios[1]

[1] Institute of Sound and Vibration Research, University of Southampton,
Highfield Campus, Southampton, SO17 1BJ, UK
e-mail: {S.G.Koroma,E.Ntotsios}@soton.ac.uk, djt@isvr.soton.ac.uk

[2] Civil and Architectural Engineering Department, Qatar University
P.O. Box 2713, Qatar
e-mail: mhussein@qu.edu.qa

Keywords: Ground Vibration, Finite Element Method, Space-Time Domain, Wavenumber Domain.

Abstract. *In this paper, a mixed model for studying ground vibration generated from surface railway tracks is presented. A ballasted track with nonlinear resilient components is modelled in the time domain using the Finite Element method. The ground is modelled as a linear homogeneous half-space in the wavenumber domain for faster computation. The interaction between the track and the ground is incorporated into the track model through a layer of Lumped Parameter Model (LPM) representing the vertical impedance of the ground. The coefficients of the components of the LPM are obtained by curve fitting of the transfer function of the half-space for a load applied at its origin.*

The coupled equation of motion for the track/ground system is formulated with excitation from a stationary point load- consisting of static and dynamic parts- acting at the centre of the rail. The coupled equation is solved by numerical integration. The calculated interaction forces at the ballast/ground interface from the space-time domain track model are Fourier transformed to the wavenumber domain and used as excitation to the ground model in order to calculate free-field surface vibration of the ground.

Results are presented for the vertical dynamic impedance for the ground, track and ground displacement in the vicinity of the track and in the free-field. A comparative study between the mixed formulation with the LPM for the ground, and a fully coupled wavenumber domain model is conducted for linear parameters. Using the fully coupled model as a benchmark, it has been observed that the inclusion of the lumped parameter ground model in the track model gives good estimation of the transmitted forces, and hence ground vibration, both in the near and far fields. Finally, the effect of nonlinear track components is briefly investigated for different levels of static preload.

1 INTRODUCTION

The numerical modelling of ground vibration from surface railways has been the focus of many researches over the years. When linear parameters are used considered for the track and ground, the modelling can be readily done in the frequency-wavenumber domain, e.g. [1, 2]. However, time domain techniques such as Finite Element (FE) and Boundary Elements (BE) are necessary for this problem when non-linear components and/ or complex irregular geometries are to be modelled, e.g. [3]. The use of FE and BE methods can be very costly indeed in terms of the computational hardware and time required for the simulations. This is mainly due to the sheer number of elements required to discretise the ground.

An alternative, which is widely used in soil-structure interaction problems, e.g. vibration of machine foundation on a half-space, is to represent the ground as approximate Lumped Parameter Models (LPM) of spring, dashpot and mass elements. This approach has been applied to ground vibration from surface trains by [4, 5]. The LPM is formulated based on Lysmer's analog fitting which, due to its simplicity, is mostly accurate for modelling the asymptotic values of the dynamic impedance at low and high frequencies, without capturing mid frequency fluctuations. A systematic approach for formulating consistent LPM with real, frequency independent coefficients, to represent an unbounded soil medium was presented in [6, 7]. In this approach, each dynamic stiffness coefficient in the frequency domain; e.g. the vertical impedance due to a vertical load, can be represented in discrete form as a rational fraction. This is subsequently decomposed into singular, first- and second-order parts, depending on the nature of the roots of the rational fraction. These models can provide high degree of accuracy when sufficiently high order of approximating polynomials are used. They also have the advantage of being incorporated in standard FE/BE routines with the possibility of including nonlinear parameters in the structure.

In this paper, a mixed space-time and wavenumber domain approach for predicting ground vibration is presented. In Section 2, an LPM for a halfspace subjected to a rectangular loading is formulated by fitting the vertical dynamic impedance calculated in the wavenumber-frequency domain. This model is then used in a time domain nonlinear FE model of a railway track, presented in Section 3, in order to calculate the dynamic track/ground interaction forces. Once these forces are obtained, they can be transformed to the wavenumber domain and used as input for predicting surface ground vibration in the far-field. The procedure for doing this is briefly discussed in Section 4. Results are presented in Section 5 which show the validity of the method and to study the influence of track nonlinearity on the predicted ground vibration.

2 MODELLING OF THE GROUND

The ground is modelled as a homogeneous elastic half-space in the wavenumber-frequency domain. The excitation is a harmonic load distributed over a rectangular area and centred about the origin of the half-space. The wavenumber-frequency domain representation of the vertical impedance of the ground is presented in Section 2.1. The approximate LPM for this impedance function is formulated in Section 2.2.

2.1 Wavenumber-domain modelling of the ground

Figure 1 shows a 3D model of a half-space that represents the ground. A harmonic rectangular load acts about its origin with dimensions $2a$ and $2b$ in the x and y directions respectively. The formulation for this problem was presented by [1].

The distributed force on the rectangular area is defined as $F_0(x,y)\mathrm{e}^{\mathrm{i}\omega t}$, where $F_0(x,y)$ is

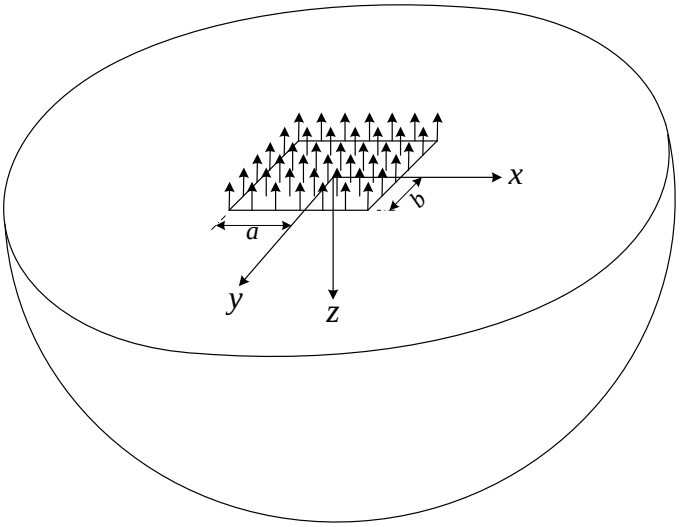

Figure 1: Ground modelled as a 3D half-space and subjected to a rectangular load.

related to the total point force, F_g, by

$$F_0(x,y) = \begin{cases} F_g/4ab, & |x| < a \quad \text{and} \quad |y| < b, \\ 0, & \text{elsewhere} \end{cases}. \tag{1}$$

The complex amplitude of the displacement of the ground in the wavenumber domain can be expressed as

$$\tilde{U}_g(\xi,\gamma,\omega) = \tilde{H}_g(\xi,\gamma,\omega) F_g \frac{\sin \xi a \sin \gamma b}{\xi a \gamma b}, \tag{2}$$

where $\tilde{H}_g(\xi,\gamma,\omega)$ is the displacement of the ground at the origin due to the total force, F_g, concentrated at the origin. $\tilde{H}_g(\xi,\gamma,\omega)$ is given by [8]

$$\tilde{H}_g(\xi,\gamma,\omega) = \frac{1}{\mu}\left[\frac{\eta_3\left(\xi^2+\gamma^2-\eta_1^2\right)}{\left(\xi^2+\gamma^2+\eta_1^2\right)^2 - 4\eta_1\eta_3\left(\xi^2+\gamma^2\right)}\right], \tag{3}$$

where $\eta_1 = -\sqrt{\xi^2+\gamma^2-\omega^2/v_s^2}$, $\eta_3 = -\sqrt{\xi^2+\gamma^2-\omega^2/v_p^2}$; for $\Re(\eta_1) \leq 0$ and $\Re(\eta_1) \leq 0$, $v_p^2 = (\lambda+2\mu)/\rho$, $v_s^2 = \mu/\rho$; with v_p and v_s being the pressure and shear wave speeds respectively, λ and μ the Lamé constants and ρ the soil density.

By transforming Eq. (2) from the wavenumber to the space domain using the double inverse Fourier transforms, the displacement in the space is obtained as

$$u_g(x,y,\omega) = \frac{F_g}{4\pi^2}\int_{-\infty}^{\infty}\int_{-\infty}^{\infty} \tilde{H}_g(\xi,\gamma,\omega)\frac{\sin \xi a \sin \gamma b}{ab\xi\gamma} \mathrm{e}^{\mathrm{i}(\xi x+\gamma y)} \mathrm{d}\xi \mathrm{d}\gamma. \tag{4}$$

The vertical dynamic impedance $k_g(x,y,\omega)$ is the ratio of the input force to the displacement and can therefore be written as

$$k_g(x,y,\omega) = \frac{4\pi^2}{\int_{-\infty}^{\infty}\int_{-\infty}^{\infty} \tilde{H}_g(\xi,\gamma,\omega)\frac{\sin \xi a \sin \gamma b}{ab\xi\gamma} \mathrm{e}^{\mathrm{i}(\xi x+\gamma y)} \mathrm{d}\xi \mathrm{d}\gamma}. \tag{5}$$

In the next section, the LPM that approximately models the impedance function in Eq. 5 will be formulated.

2.2 Lumped parameter representation of the ground

The objective of this section is to formulate an LPM with spring and dashpot components having real frequency independent coefficients [6, 7], to approximately model the dynamic impedance function in Eq. (5). Suppose that Eq. (5) can be represented in discrete form as sum of its singular part, $\bar{K}_s(\mathrm{i}\omega)$, and remaining regular part, $\bar{K}_r(\mathrm{i}\omega$. The singular part, $\bar{K}_s(\mathrm{i}\omega) = k_0 + \mathrm{i}\omega c_0$, describes its asymptotic value at high frequencies. The regular part, $\bar{K}_r(\mathrm{i}\omega)$ can be expressed as a rational fraction with numerator having order 1 less than the denominator. Hence, the discrete dynamic impedance, $\bar{K}(\mathrm{i}\omega)$ can be summarised as

$$\bar{K}(\mathrm{i}\omega) = \underbrace{k_0 + \mathrm{i}\omega c_0}_{\text{singular part}} + \underbrace{\frac{1 + p_1(\mathrm{i}\omega) + p_2(\mathrm{i}\omega)^2 + \cdots + p_{M-1}(\mathrm{i}\omega)^{M-1}}{1 + q_1(\mathrm{i}\omega) + q_2(\mathrm{i}\omega)^2 + \cdots + q_M(\mathrm{i}\omega)^M}}_{\text{regular part}} \tag{6}$$

where p_i and q_i are the $2M-1$ unknown real coefficients to be determined by numerical curve fitting. The regular part, $\bar{K}_r(\mathrm{i}\omega)$ can be alternatively represented using partial fraction expansion as

$$\bar{K}_r(\mathrm{i}\omega) = \sum_{l=1}^{M} \frac{A_l}{\mathrm{i}\omega - s_l}, \tag{7}$$

where s_l and A_l are the poles and corresponding residues of $\bar{K}_r(\mathrm{i}\omega)$. Note that for a stable system, each s_l should have a negative real part, and this condition can be achieved by adopting an iterative procedure in the curve fitting routine. The poles of $\bar{K}_r(\mathrm{i}\omega)$ can be all real, all complex conjugate pairs or a combination of these. A real pole results in a first-order approximation term with corresponding real coefficients whereas a pair of complex conjugate poles, when added together, form a second-order approximation term with real coefficients. For J complex conjugate pairs and the remaining $M-2J$ real poles, the dynamic stiffness for the generalised LPM can be written in parallel form that includes all the sub components as

$$\bar{K}(\mathrm{i}\omega) = k_0 + \mathrm{i}\omega c_0 + \sum_{l=1}^{J} \frac{\beta_{1l}\mathrm{i}\omega + \beta_{0l}}{(\mathrm{i}\omega)^2 + \alpha_{1l}\mathrm{i}\omega + \alpha_{0l}} + \sum_{l=1}^{M-2J} \frac{A_l}{\mathrm{i}\omega - s_l}, \tag{8}$$

The coefficients of the second-order term are as follows

$$\alpha_{0l} = \prod_{i=j}^{j+1} s_i, \quad \alpha_{1l} = -\sum_{i=j}^{j+1} s_i, \quad \beta_{0l} = -(A_j s_{j+1} + A_{j+1} s_j), \quad \beta_{1l} = \sum_{i=j}^{j+1} A_i,$$

where $j \in \{1, 3, \cdots, 2J-1\}$ and $j+1$ form a pair of complex conjugates of poles and of corresponding residues at those poles.

Figure 2 shows the generalised LPM, with the components marked (I), (II) and (III) being the singular part, first-order terms and second-order terms of the regular part respectively. The coefficients of the first and second order terms are derived in [6] as being related to the poles and residues of $\bar{K}_r(\mathrm{i}\omega)$ as follows

$$k_{1,l} = \frac{A_l}{s_l}, \quad c_{1,l} = -\frac{A_l}{s_l^2}, \quad k_{2,j} = -\frac{\beta_{0l}}{\alpha_{0l}}, \quad c_{2,j} = \frac{\alpha_{0l}\beta_{1l} - \alpha_{1l}\beta_{0l}}{\alpha_{0l}^2},$$
$$k_{2,j+1} = \frac{\beta_{0l}(-\alpha_{0l}\beta_{1l} + \alpha_{1l}\beta_{0l})^2}{\alpha_{0l}^2(\alpha_{0l}\beta_{1l}^2 - \alpha_{1l}\beta_{0l}\beta_{1l} + \beta_{0l}^2)}, \quad c_{2,j+1} = \frac{\beta_{0l}^2(-\alpha_{0l}\beta_{1l} + \alpha_{1l}\beta_{0l})}{\alpha_{0l}^2(\alpha_{0l}\beta_{1l}^2 - \alpha_{1l}\beta_{0l}\beta_{1l} + \beta_{0l}^2)}.$$

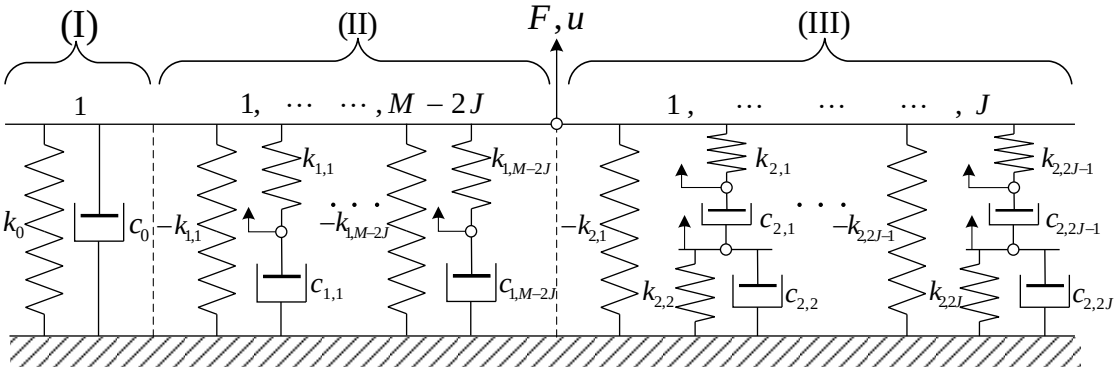

Figure 2: Lumped parameter ground model approximation for a half-space

The force-displacement relationship of the generalised LPM can be expressed in matrix form as

$$\left\{F_g\right\} = \left[C_g\right]\left\{\dot{U}_g\right\} + \left[K_g\right]\left\{U_g\right\}, \tag{9}$$

where

$$K_g = \begin{bmatrix} k_0 & -k_{1,1} & \cdots & -k_{1,M-2J} & -k_{2,1} & 0 & \cdots & \cdots & -k_{2,2J-1} & 0 \\ -k_{1,1} & k_{1,1} & & & & & & & & \\ \vdots & & \ddots & & & & & & & \\ -k_{1,M-2J} & & & k_{1,M-2J} & & & & & & \\ -k_{2,1} & & & & k_{2,1} & & & & & \\ 0 & & & & & k_{2,2} & & & & \\ \vdots & & & & & & \ddots & & & \\ \vdots & & & & & & & \ddots & & \\ -k_{2,2J-1} & & & & & & & & k_{2,2J-1} & \\ 0 & & & & & & & & & k_{2,2J} \end{bmatrix},$$

$$C_g = \begin{bmatrix} c_0 & & & & & & & & & \\ & c_{1,1} & & & & & & & & \\ & & \ddots & & & & & & & \\ & & & c_{1,M-2J} & & & & & & \\ & & & & c_{2,1} & -c_{2,1} & & & & \\ & & & & -c_{2,1} & c_{2,1}+c_{2,2} & & & & \\ & & & & & & \ddots & \ddots & & \\ & & & & & & \ddots & \ddots & & \\ & & & & & & & & c_{2,2J-1} & -c_{2,2J-1} \\ & & & & & & & & c_{2,2J-1} & c_{2,2J} \end{bmatrix},$$

and $\left\{U_g\right\}^T = \left\{u_0,\ \ u_1,\ \ \cdots,\ \ u_{M-2J},\ \ u_{M-2J+1}, \cdots\ \ \cdots\ \ , u_M\right\}$. Equation (9) can be directly used in coupling a structure to the ground, as will be described for the case of a railway track in the next section.

3 SPACE-TIME DOMAIN MODELLING OF THE TRACK

3.1 Model description

Fig. 3 shows a model of a ballasted railway track. The model comprises of rail discretely supported on sleepers via railpads. The sleepers are resting on ballast which is in turn resting on the ground. The rail is modelled as an Euler-Bernoulli beam of mass, m_r, per unit length and

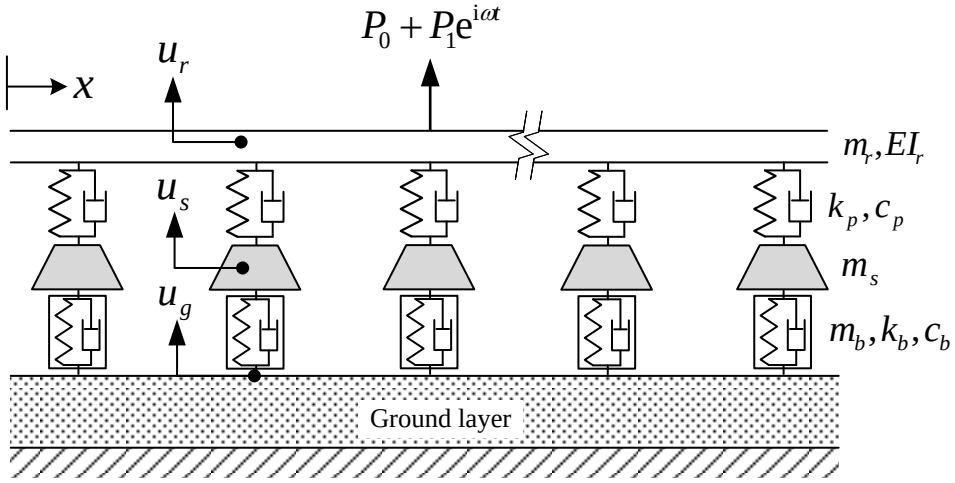

Figure 3: Model of a ballasted railway track on supporting ground layer, excited by a moving vehicle on irregular rail surface

bending stiffness, EI. The railpads are modelled as nonlinear with preload dependent stiffness and damping, k_p and c_p respectively. The sleepers are modelled as lumped masses, m_s, having only vertical translation. At each sleeper position, the ballast is modelled as having a mass, m_b, consistently distributed between the sleeper and ground nodes, stiffness and damping, k_b and c_b respectively. The LPM formulated in the previous section to represent the ground, is coupled to the each sleeper node. It should be noted that appropriate scaling of the LPM needs to be done to correctly account for the sleeper spacing.

3.2 Equation of motion of the track/ground model

The differential equation for the coupled track/ground model is given by

$$\begin{bmatrix} \mathbf{M}_r & \mathbf{0} & \mathbf{0} \\ \mathbf{0} & \mathbf{M}_s + \mathbf{M}_b^{ss} & \mathbf{M}_b^{sg} \\ \mathbf{0} & \mathbf{M}_b^{gs} & \mathbf{M}_b^{gg} \end{bmatrix} \begin{Bmatrix} \ddot{\mathbf{U}}_r \\ \ddot{\mathbf{U}}_s \\ \ddot{\mathbf{U}}_g \end{Bmatrix} + \begin{bmatrix} \mathbf{C}_p^{rr} & \mathbf{C}_p^{rs} & \mathbf{0} \\ \mathbf{C}_p^{sr} & \mathbf{C}_p^{ss} + \mathbf{C}_b^{ss} & \mathbf{C}_b^{sg} \\ \mathbf{0} & \mathbf{C}_b^{gs} & \mathbf{C}_b^{gg} \end{bmatrix} \begin{Bmatrix} \dot{\mathbf{U}}_r \\ \dot{\mathbf{U}}_s \\ \dot{\mathbf{U}}_g \end{Bmatrix} + \begin{bmatrix} \mathbf{K}_r + \mathbf{K}_p^{rr} & \mathbf{K}_p^{rs} & \mathbf{0} \\ \mathbf{K}_p^{sr} & \mathbf{K}_p^{ss} + \mathbf{K}_b^{ss} & \mathbf{K}_b^{sg} \\ \mathbf{0} & \mathbf{K}_b^{gs} & \mathbf{K}_b^{gg} \end{bmatrix} \begin{Bmatrix} \mathbf{U}_r \\ \mathbf{U}_s \\ \mathbf{U}_g \end{Bmatrix} = - \begin{Bmatrix} \mathbf{F}_r \\ \mathbf{0} \\ \mathbf{F}_g \end{Bmatrix}, \tag{10}$$

where $\mathbf{M}_{\{.\}}$, $\mathbf{C}_{\{.\}}$, $\mathbf{K}_{\{.\}}$ and $\mathbf{U}_{\{.\}}$ are the global mass, damping and stiffness matrices and displacement vector of the track components indicated by the subscripts, r, s, b and g, for the rail, sleeper, ballast and ground respectively. The superscripts on the other hand designate cross-coupling between these components. $\mathbf{F}_r$ is the external nodal force vector of the rail due to the

excitation force and $\mathbf{F}_g$ is the interaction force vector at the ballast/ground interface. $\mathbf{F}_g$ is the global assembly of all the ground nodes, each represented by Eq. (9). Since the ground displacements are also unknowns, direct substitution of $\mathbf{F}_g$ results in a modification to the global damping and stiffness matrices of the track/ground model.

3.3 Nonlinear railpad and ballast properties

As stated earlier, the railpad and ballast properties are modelled as generally nonlinear with preload dependent stiffness and damping properties. The static force-displacement behaviour of the railpad and ballast can be approximated by polynomials of degree α and β respectively,

$$f_{ps}(u_{ps}) = k_{p,1}u_{ps} + k_{p,2}u_{ps}^2 + \cdots + k_{p,\alpha}u_{ps}^{\alpha} \tag{11a}$$

$$f_{bs}(u_{bs}) = k_{b,1}u_{bs} + k_{b,2}u_{bs}^2 + \cdots + k_{b,\beta}u_{ps}^{\beta} \tag{11b}$$

where f_{ps}, u_{ps} and $k_{p,1} \cdots k_{p,\alpha}$ are the static force (in Newton), displacement (in metre) and stiffness coefficients of the railpad respectively. f_{bs}, u_{bs} and $k_{b,1} \cdots k_{b,\beta}$ are the corresponding values for the ballast. For the railpad, the values of the non zeros coefficients are $k_{p,1} = 20.00$ MN/m, $k_{p,3} = 3.94 \times 10^6$ MN/m^3, $k_{p,5} = -1.78 \times 10^{12}$ MN/m^5 and $k_{p,7} = 3.28 \times 10^{18}$ MN/m^7 [9], and for the ballast, $k_{b,1} = 22.75$ MN/m and $k_{b,3} = 2.6 \times 10^8$ MN/m^3 [10]. Note that when the track is fully unloaded, the railpad and ballast possess unloaded stiffness of $k_{p,1}$ and $k_{b,1}$ respectively.

3.4 Solution of the coupled equation of motion

Under the action of the static load, the preloads and hence the preloaded stiffness of the railpads and ballast are calculated by solving the nonlinear static equivalent of Eq. (10) using Newton-Raphson iterative routine. These are then used as input values for the dynamic part of the problem, defined by Eq. (10). The solution for the track and ground displacements and the interaction forces at the ballast/ground interface are obtained by by progressive numerical integration.

The calculated interaction forces at the ballast/ground are then used as input to calculate ground vibration in the far-field. This process is described in the next section.

4 FREE-FIELD GROUND VIBRATION CALCULATION

Using the computed displacement and its derivatives, the interaction forces at the ballast/ground interface can also be computed. For this problem, all sleeper and hence ground nodes vibrate with the same frequency as the load. Therefore it is sufficient to consider only the complex amplitude of the interaction force in the space-time domain. This is given as

$$F_g(x_s) = |\mathbf{F}_g(x_s, t)| = |\mathbf{C}\dot{\mathbf{U}}_g + \mathbf{K}_p\mathbf{U}_g|. \tag{12}$$

The non-zero forces of $F_g(x_s)$ occur at the ground nodes that are coupled to the sleepers, with the internal nodes of the LPM being zeros. These non-zero forces are assembled in a new vector, $\bar{F}_g(x_s)$, with size $2n_s + 1 \times 1$, where n_s and x_s are the number of sleepers and sleeper positions respectively. It is convenient to convert $\bar{F}_g(x_s)$ to piecewise continuous function, $\bar{F}'_g(x)$, using linear shape functions.

The spatial Fourier transformation of $\bar{F}'_g(x)$ to the wavenumber domain can be obtained from

$$\hat{\bar{F}}'_g(\xi) = \int_{-\infty}^{\infty} \bar{F}'_g(x)\mathrm{e}^{-\mathrm{i}\xi x}\mathrm{d}x. \tag{13}$$

The complex amplitude of the ground displacement in the wavenumber domain is therefore given by

$$\tilde{U}'_g(\xi,\gamma,\omega) = \tilde{H}_g(\xi,\gamma,\omega)\hat{\tilde{F}}'_g(\xi)\frac{\sin\gamma b}{\gamma b}. \tag{14}$$

The corresponding displacement in the space-time domain is obtained by applying the double inverse Fourier transformation as follows

$$u'_g(x,y,\omega) = \frac{1}{4\pi^2}\int_{-\infty}^{\infty}\int_{-\infty}^{\infty}\tilde{H}_g(\xi,\gamma,\omega)\hat{\tilde{F}}'_g(\xi)\frac{\sin\gamma b}{\gamma b}\mathrm{e}^{\mathrm{i}(\xi x+\gamma y)}\mathrm{d}\xi\mathrm{d}\gamma. \tag{15}$$

In the next section, numerical results will be presented to show the validity of this approach and to investigate the effect of nonlinear track properties on ground vibration.

5 RESULT AND DISCUSSION

Section 5.1 presents the result of the LPM approximation of the ground dynamic impedance. The LPM is then used to study nonlinear track dynamics. Results for this application are given in Section 5.2 whereas free-field ground displacements are presented in Section 5.3.

5.1 Dynamic stiffness of the LPM

The following parameters are used for the ground: $\rho = 1800$ kg/m^3, $v_s = 245$ m/s and $v_p = 750$ m/s and damping ratio of 5%.

The vertical dynamic stiffness from Eq. (5) is computed using $b = 1.35$ m and an optimal a value of 0.724 m. For the LPM approximation, polynomials of order 6 and 7 for the numerator and denominator respectively are used. This results in one real and three complex conjugate pair poles, hence the LPM consists of one first-order and three second-order terms. These are then arranged in parallel with the singular part of spring, $k_0 = -12.853$ and dashpot, $c_0 = 2.569$. The values of the coefficient of the components of the LPM are given in Table 1.

Table 1: Coefficients of the components of the LPM

j	$k_{1,j}$	$c_{1,j}$	$k_{2,j}$	$k_{2,j+1}$	$c_{2,j}$	$c_{2,j+1}$
1	-16.290	-1.142	1.755	-0.381	-0.110	0.077
3			2.524	-0.141	0.108	-0.106
5			1.821	-0.067	-0.118	0.109

Figure 4 shows the real and imaginary parts of the dynamic stiffness, normalised against the static stiffness, K_0. It shows a comparison between the numerical and LPM representation. A dimensionless frequency $\bar{\omega} = \omega h/v_s$, has been adopted; where h is a characteristic length, taken as the smaller of the rectangular load dimensions a and b. It can be seen that the LPM is a good representation of the computed dynamic stiffness of the half-space.

5.2 Track and ground vibration

Table 2 contains the track parameters used in the computation of the track dynamic response and, together with the LPM model, the ground response.

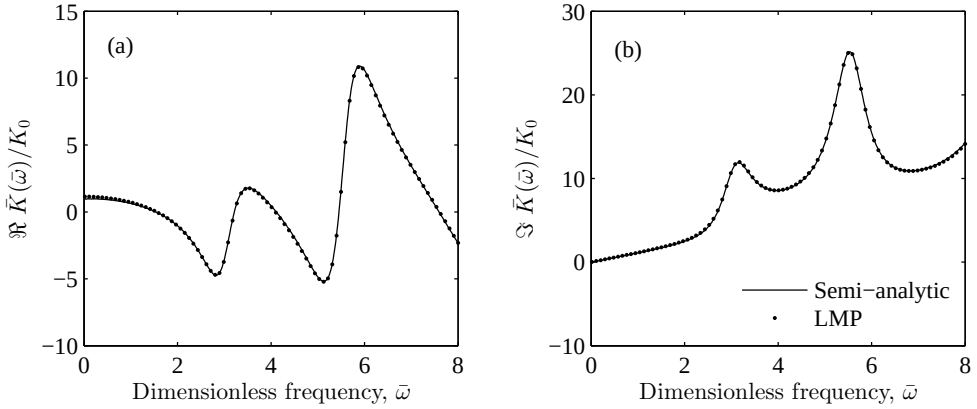

Figure 4: (a) Real and (b) imaginary parts of the dynamic stiffness of a half-space subjected to rectangular harmonic load. Comparison between the semi-analytic and LPM

Table 2: Track parameters used in the numerical study

Rail	Railpad	Sleeper	Ballast
m_r = 60.21 kg/m	ζ_p = 0.125	m_s = 250 kg/m	m_b = 870 kg/m
EI_r = 6.4 MN m^2			ζ_b = 0.50

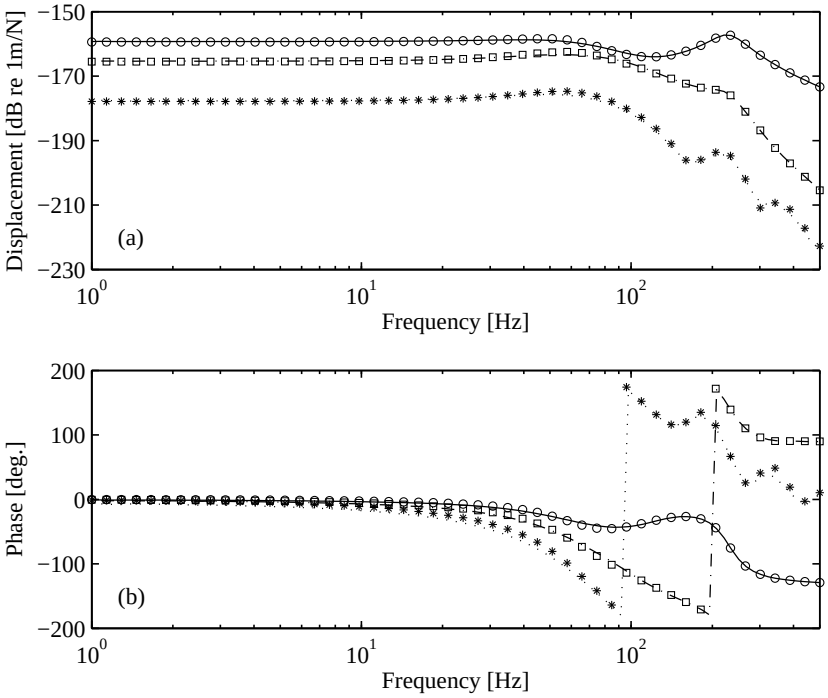

Figure 5: Displacement amplitude and phase of the rail (—,○), sleeper (-·-,□) and ground (· · ·,*), plotted against excitation frequency. Comparison between track on half-space [2] (lines) and on LPM for the ground (markers).

Figure 5 shows the variation of the rail, sleeper and ground displacement amplitude and phase at the driving point with frequency. The results obtained using the LPM is compared with that of the semi-analytic procedure for linear track parameters. For this calculation, the rail is modelled using 240 elements, each of length 0.3 m, 121 sleepers and therefore same number of ground nodes. Good agreement between the two methods can be observed. At low frequencies, the rail displacement is about 6.1 and 18.5 dB larger than the sleeper and ground displacements. Resonances can be seen to occur for the sleeper/ballast at around 48-60 Hz and for the rail at around 220 Hz. The fluctuations in the ground displacement due to the width of the ballast can also be seen.

Results will now be presented to show the effect of track nonlinearity for static loads of 0, 50, 87.5 and 125 kN. The stiffness of the railpad and ballast increases significantly with preload. Figure 6 shows the amplitude and phase of he rail, sleeper and ground displacements at the driving point, plotted against frequency for these preload levels. The effect of increasing stiffness

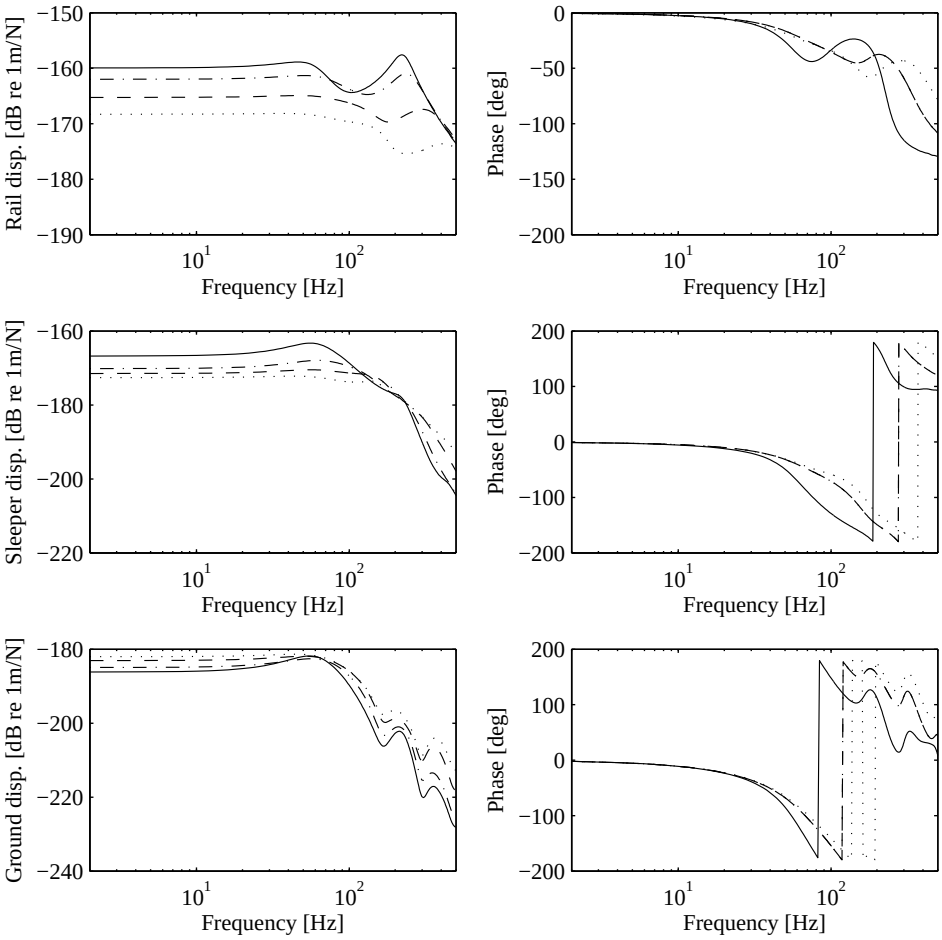

Figure 6: Displacement amplitude and phase of the rail, sleeper and ground, plotted against excitation frequency for preload levels of 0 kN —, 50 kN -·-, 87.5 kN - - -, 125 kN · · · .

of the railpad and ballast, which is a direct consequence of the preload dependence, is apparent in the figure with lower amplitudes and increased cut-on frequency observed with increase in static load. Also the preload dependence of the railpad and ballast results to higher interaction force at the ballast/ground interface and consequently leads to larger ground displacements

over a wide range of frequencies. Since the ground is linear, however, the peaks in the ground displacement occur at approximately the same frequencies for all preload levels.

5.3 Free-field ground vibration

Finally, using the interaction forces at the ballast/ground interface, free-field ground vibration can be calculated in accordance with the procedure in Section 4.
Figure 7 shows the ground displacement amplitude plotted against distance away from the track for the preload levels specified above, for a load oscillating at (a) 10 Hz and (b) 120 Hz. For

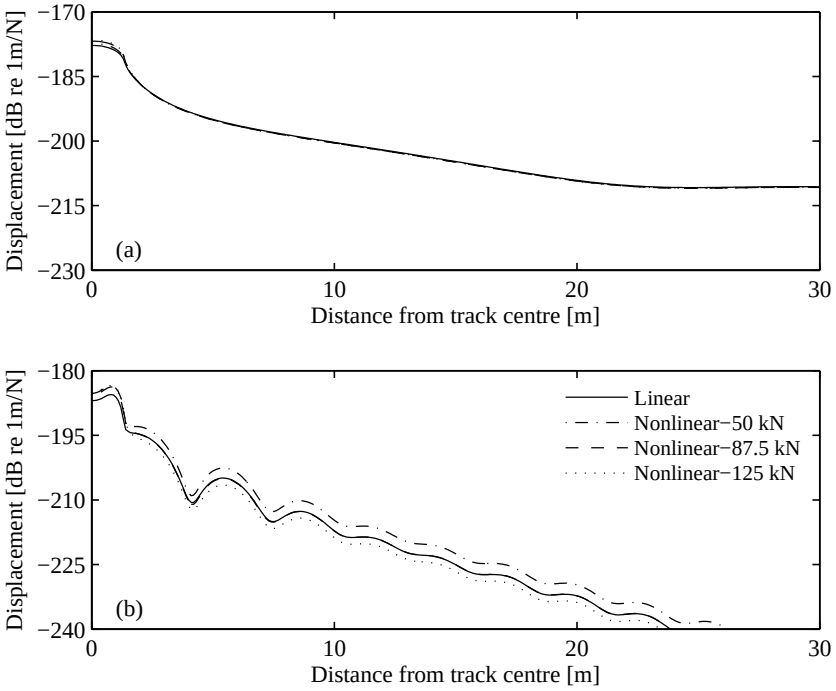

Figure 7: Variation of ground displacement amplitude with distance away from the track for the four preload levels and load frequency of (a) 10 Hz, (b) 120 Hz.

the case in (a), only small differences in the vicinity of the track can be observed, with the displacement being almost the same further away from the track. The interaction force profile of the nonlinear track is narrower than that for the linear track, so that even though its amplitudes are larger, the total transmitted force to the ground (taken as the area under the force profile) is fairly equivalent with the linear track. Larger differences of up to 3 dB can be observed, however, for the higher frequency case in (b).

6 CONCLUSIONS

This paper presents a mixed formulation involving both space-time and wavenumber domain techniques applied to the study of ground vibration from surface trains. The track is modelled in the time domain in order to include nonlinear track elements, and the ground in the wavenumber domain. For the purpose of calculating the track/ground interaction forces in the space-time domain, the ground is represented by a layer of consistent lumped parameter model consisting of frequency independent stiffness and damping components. The calculated interaction forces

are then transformed to the wavenumber domain and used as input to study ground vibration in the far field. For the example case presented, the LPM model shows good comparison with the fully coupled track-ground model. The effect of nonlinearity on ground vibration has been found to be significant mostly in the vicinity of the track but not in the far field, with differences of up to 3 dB observed between the linear and the highly nonlinear cases.

ACKNOWLEDGEMENTS

This work is undertaken as part of the MOTIV (Modelling of Train Induced Vibration) project which is funded by the EPSRC under grant EP/K005847/2.

REFERENCES

[1] D.V. Jones, D. Le Houedec, M. Petyt, Ground vibrations due to a rectangular harmonic load. *Journal of Sound and Vibration*, **212**, 67-74, 1998.

[2] X. Sheng, C.J.C. Jones, M. Petyt, Ground vibration generated by a harmonic load acting along a railway track. *Journal of Sound and Vibration*, **225**, 3-28, 1999.

[3] P.A. Costa, R. Calçada, A.S. Cardoso, A. Bodare, Influence of soil non-linearity on the dynamic response of high-speed railway tracks. *Soil Dynamics & Earthquake Engineering*, **30**, 221-235, 2010.

[4] G. Kouroussis, G. Gazetas, I. Anastasopoulos, C. Conti, O. Verlinden, Discrete modelling of vertical track-soil coupling for vehicle-track dynamics. *Soil Dynamics & Earthquake Engineering*, **192**, 1711-1723, 2011.

[5] G. Kouroussis, O. Verlinden, C. Conti, A two-step time simulation of ground vibrations induced by the railway traffic. *Proceedings of the Institution of Mechanical Engineers, Part C: Journal of Mechanical Engineering Science*, **226**, 454-472, 2012.

[6] J.P. Wolf, Consistent lumped-parameter models for unbounded soil: Physical representation. *Soil Dynamics & Earthquake Engineering*, **20**, 11-32, 1991.

[7] J.P. Wolf, Consistent lumped-parameter models for unbounded soil: Frequency-independent stiffness, damping and mass matrices. *Soil Dynamics & Earthquake Engineering*, **20**, 33-41, 1991.

[8] K.F. Graff, *Wave Motion in Elastic Solids*. Dover publications, inc., 1991.

[9] S.G. Koroma, M.F.M. Hussein, J.S. Owen, The effects of railpad nonlinearity on the vibration of railway tracks under harmonic load. Z. Dimitrovová, J.R. de Almeida, R. Gonçalves eds. *11th International Conference on Vibration Problems (ICOVP-2013)*, Lisbon, Portugal, September 9-12, 2013.

[10] T.X. Wu, D.J. Thompson, The effects of track non-linearity on wheel/rail impact. *Proceedings of the Institution of Mechanical Engineers, Part F: Journal of Rail and Rapid Transit*, **218**, 1-15, 2004.